International Journal of Signal Processing, Image Processing and Pattern Recognition
Vol.8, No.3 (2015), pp.261-272
http://dx.doi.org/10.14257/ijsip.2015.8.3.24

Kernel based Digital Image Correlation

Huan Shen[1, 2,*], Peize Zhang[1], and Xiang Shen[2]

[1] *Energy and Power College, Nanjing University of Aeronautics and Astronautics, No. 29, Yudao Street, Baixia District, Nanjing 210016, China*
[2] *Aeronautics Science and Technology Key Laboratory of full scale aircraft structure and fatigue, No. 85, Dianzi 2nd Road, Yanta District, Xi'an 710065, China*
**Huan Shen: huan_shen@nuaa.edu.cn*

Abstract

Digital image correlation (DIC) is an effective displacement field measurement method featuring non-contact and full-field, which has been successfully applied in lots of fields, especially in the field of experimental mechanics. Unfortunately, the traditional DIC technique (TDIC) depends on the output values of image sensor heavily that usually noised in practical imaging system. So, TDIC cannot deal with bias error introduced by the image noise effectively. In this paper, a kernel based DIC is proposed to help reduce the bias error by establishing and optimizing a weighted correlation function. Compared with the methods of low-pass filtering, KDIC preserves the high frequency information well but reduces the bias error caused by image noise effectively. To demonstrate, two kinds of kernel function are analyzed. One is Epanechnikov kernel, with which KDIC is equivalent to TDIC. The other is Gaussian kernel, which can be used to improve the anti-noise performance of TDIC and get more accurate sub-pixel displacements. Both simulation analyses and experimental results validate the effectiveness of this new method.

Keywords: *Kernel; Bias error reduction; Image noise; Digital image correlation*

1. Introduction

Digital image correlation (DIC) is a novel technique widely used especially in the field of experimental mechanics due to its advantages, such as non-contact measurement, simpleness of building the system, more accurate testing results and so on [1-5]. DIC uses digital images recorded by almost any image acquisition device as input and full-field displacements in subpixel as output. Then, full-field strain distributions can be further differentiated by the obtained full-field displacements via appropriate numerical differentiation methods [6-7]. Obviously, accurate displacements are the bases for subsequent analyses. With this considered, lots of effort is made to study on the factors like speckle pattern, image subset size, correlation function, interpolation algorithms and so on [8-11]. Some researchers have proposed some principles and suggestions for high accuracy DIC calculation.

However, for DIC application in real experiments, not much work is launched to deal with the inevitable random noise in the experimental images. Theoretical analyses have indicated that random noise can affect the intensity distribution of the images and introduce both bias error and variance [12] in the displacement estimation that is basically extracted from the intensity information of the images before and after deformation. At the same time, some researchers have demonstrated that a larger subset in DIC can dramatically reduce the variance of the displacement distribution, but has no effect on the bias error [13]. Some researchers suggest preprocessing the image for denoising [14-16], for example, Pan [13] proposed a pre-

ISSN: 2005-4254 IJSIP

smoothing method to deal with the noisy images with a Gaussian low-pass filter for bias error reduction. Nevertheless, Gaussian filter means image fuzzification, undoubtedly reducing the intensity gradient, which may lead to greater variance of the displacement estimation. More importantly, optimal kernel size of the filter is uncertain. It needs to be determined artificially but with real deformation parameters unknown in practical experiments.

In this paper, influences of the noise level on the displacement estimation calculated by the traditional DIC that is with low noise immunity are investigated. Then, a kernel based digital image correlation method (KDIC) is given to process the noisy images and reduce the bias error in the displacement without changing the deformation carrier intensity but optimizing the algorithm itself for high-precision measurement in real experiments. Both the simulation results and the experimental analyses validate the effectiveness and robustness of the KDIC technique that is insensitive to the image noise.

2. Introductions of TDIC and KDIC

2.1. Basic Principles of TDIC

Principles of TDIC are very simple. Deformation measurement, such as displacement estimation, strain distribution of the structure surface and so on, can be transformed into matching the images of the structure before and after deformation. Firstly, the shape function is built to describe deformation of the structure. With an arbitrary point (x, y) and its neighbourhood S called reference subset given, a mapping relation χ satisfies

$$\chi(x,y)\to(\tilde{x},\tilde{y}),\ f(x,y)=g(\tilde{x},\tilde{y})$$

Where $f(x,y)$ represents the intensity of the image before deformation at point (x, y); $g(\tilde{x},\tilde{y})$ stands for the intensity of the image after deformation at point $(\tilde{x},\tilde{y})$.

Mapping relation χ is the so-called shape function. If neighbourhood S is small enough, then χ can be described as

$$\begin{aligned}\tilde{x} &= x+u(x_0,y_0)+\frac{\partial u}{\partial x}\Big|_{x_0,y_0}(x-x_0)+\frac{\partial u}{\partial y}\Big|_{x_0,y_0}(y-y_0)\\ \tilde{y} &= x+v(x_0,y_0)+\frac{\partial v}{\partial x}\Big|_{x_0,y_0}(x-x_0)+\frac{\partial v}{\partial y}\Big|_{x_0,y_0}(y-y_0)\end{aligned} \quad (1)$$

Where u and v are the in plane displacement in x and y direction separately; $(\frac{\partial u}{\partial x},\frac{\partial u}{\partial y},\frac{\partial v}{\partial x},\frac{\partial v}{\partial y})$ are the displacement gradient; (x_0,y_0) is the center of S.

Parameters in the shape function can be assembled as a vector:

$$P=\left(u,v,\frac{\partial u}{\partial x},\frac{\partial v}{\partial x},\frac{\partial u}{\partial y},\frac{\partial v}{\partial y}\right)$$

Then the correlation function, including deformation parameters, can be defined as

$$\rho=\frac{\sum_{s_p\in S}\left[f(s_p)-g(s_p,P)\right]^2}{\sum_{s_p\in S}f^2(s_p)} \quad (2)$$

Nonlinear optimization method is used to solve Eq.2 and the vector P can be gotten.

According to Eq.2, when the correlation function is minimized, image subset after deformation is most similar to that before deformation. Then parameters u and v in vector P

are the optimum estimation of the displacement of the structure surface. Same processing procedure will be applied to all the grid points for full-field displacement estimation.

Correlation function ρ can be minimized by Newton-Raphson method which is recommended by lots of references [1-5]. The iteration equation can be defined as

$$\boldsymbol{P} = \boldsymbol{P}_0 - \frac{\nabla\rho(\boldsymbol{P}_0)}{\nabla\nabla\rho(\boldsymbol{P}_0)} \quad (3)$$

Where P_0 is the initial value of the deformation parameter vector; $\nabla\rho$ presents the gradient of correlation function ρ; $\nabla\nabla\rho$ is the so called Hessian matrix, which is the second spatial deviation of ρ. $\nabla\rho$ and $\nabla\nabla\rho$ are shown in the following.

$$\begin{aligned}\nabla\rho &= \left(\frac{\partial\rho}{\partial P_i}\right)_{i=1,\cdots,6} \\ &= \frac{-2}{\sum_{s_p\in S} f^2(s_p)}\left\{\sum_{s_p\in S}\left[f(s_p)-g(s_p,P)\right]\frac{\partial g(s_p,P)}{\partial P_i}\right\}_{i=1,\cdots,6}\end{aligned} \quad (4)$$

$$\begin{aligned}\nabla\nabla\rho &= \left(\frac{\partial^2\rho}{\partial P_i\partial P_j}\right)_{\substack{i=1,\cdots,6\\ j=1,\cdots,6}} \\ &\approx \frac{2}{\sum_{s_p\in S} f^2(s_p)}\left\{\sum_{s_p\in S}\frac{\partial g(s_p,P)}{\partial P_i}\frac{\partial g(s_p,P)}{\partial P_j}\right\}_{\substack{i=1,\cdots,6\\ j=1,\cdots,6}}\end{aligned} \quad (5)$$

From Eq.3 to Eq.5 we can know that, component $f(s_p)-g(s_p,P)$ and $\frac{\partial g(s_p,P)}{\partial P_i}$ in the expression ρ affect the iteration results enormously. If there is no noise in the image, parameters of the shape function will approach to the true values along gradient direction per iteration procedure. When the terminal condition is satisfied, expression $\sum_{s_p\in S}\left[f(s_p)-g(s_p,P)\right]\frac{\partial g(s_p,P)}{\partial P_i}$ will tend to 0. However, if the image is contaminated by noise, component $f(s_p)-g(s_p,P)$ will not converge to zero, and component $\frac{\partial g(s_p,P)}{\partial P_i}$ will be amplified. So, results gained by TDIC are not that accurate because of image noise.

2.2. Definition of KDIC

Kernel function is added to the correlation function to improve anti-noise performance of the traditional DIC. Usually, kernel function is defined as some kind of radially symmetric scalar function called Radial Basis Function (RBF), which satisfies

$$K(x) = c_{k,d}\,k\left(\|x\|^2\right) \quad (6)$$

where, $c_{k,d}$ is normalization constant, and k is the so-called profile of corresponding kernels.

Considering the control ability of the kernel function in radial direction, intensity differences of the images before and after deformation in given neighborhood S are transformed into the feature space centered at zero. New correlation function based on kernel can be defined as

$$\rho^* = c\sum_{s_p \in S} k\left(\left\|\frac{f(s_p) - g(s_p, p)}{h}\right\|^2\right) \quad (7)$$

Where c is the normalization constant; $h(h=\sigma)$ presents the bandwidth of the kernel.

Supposed that $r(s_p, p) = f(s_p) - g(s_p, p)$, then Eq.7 can be simplified as

$$\rho^* = c\sum_{s_p \in s} k\left(\left\|\frac{r(s_p, p)}{h}\right\|^2\right) \quad (8)$$

First-order gradient of ρ^* and the Hessian matrix are shown as follows:

$$\begin{aligned}\nabla\rho^*(p) &= \left(\frac{\partial\rho^*}{\partial p_i}\right)_{i=1,\ldots,7} \\ &= -\frac{2c}{h}\left\{\sum_{s_p \in s} k'\left(\left\|\frac{r(s_p, p)}{h}\right\|^2\right)\cdot r(s_p, p)\cdot\frac{\partial g(s_p, p)}{\partial p_i}\right\}_{i=1,\ldots,6}\end{aligned} \quad (9)$$

$$\begin{aligned}\nabla\nabla\rho^*(p) &\approx \left(\frac{\partial^2\rho^*}{\partial p_i \partial p_j}\right)_{\substack{i=1,\ldots,6\\ j=1,\ldots,6}} \\ &= \frac{2c}{h}\left\{\sum_{s_p \in s} k'\left(\left\|\frac{r(s_p, p)}{h}\right\|\right)^2\cdot\frac{\partial g(s_p, p)}{\partial p_i}\frac{\partial g(s_p, p)}{\partial p_j}\right\}_{\substack{i=1,\ldots,6\\ j=1,\ldots,6}}\end{aligned} \quad (10)$$

At last, Eq.9 and Eq.10 can be substituted into Eq.3. Then, the Eq.8 is minimized to get the optimum deformation parameters for full-field displacement calculation.

Compared with the gradient and Hessian matrix of the two correlation function, KDIC is a kind of weighted TDIC in format. And weight function equals to the first-order derivative of the kernel function. Therefore, different kinds of kernel functions correspond to different weighted forms. Two common kernel functions [17], one Epanechnikov kernel, the other typical Gaussian kernel, are exampled and analyzed in the following.

(a) Epanechnikov Kernel

The profile of the Epanechnikov kernel is defined as

$$k_E(x) = \begin{cases} 1-x, if\, 0 < x < 1 \\ 0, otherwise \end{cases} \quad (11)$$

According to the expression above, we can get that

$$k'_E(x) = \begin{cases} -1, if\, 0 < x < 1 \\ 0, otherwise \end{cases} \quad (12)$$

If Epanechnikov kernel is applied, KDIC is the same to TDIC in format. That is to say, TDIC is a kind of particular case of KDIC if Epanechnikov kernel is used.

(b) Gaussian Kernel

In Gaussian kernel case, the profile is

$$k_G(x) = \exp(-\frac{1}{2}x), x > 0 \quad (13)$$

And derivative of $k_G(x)$ is calculated as

$$k'_G(x) = -\frac{1}{2}\exp(-\frac{1}{2}x), x > 0 \quad (14)$$

According to Eq.9 and Eq.10, derivative of Gaussian kernel is expressed the same as original in correlation function. Gaussian kernel is expressed as

$$k\left(\left\|x - x_c\right\|\right) = \exp\left(-\frac{\left\|x - x_c\right\|^2}{2\sigma^2}\right) \quad (15)$$

Where x_c is the center of the kernel function; σ stands for the bandwidth and controls radial actuating range of the kernel function. If x is far from the center x_c, then the function value will be small. On the contrary, small distance difference between x and x_c means a high function value.

Gaussian kernel is applied in this paper. So, in iteration Eq.3, except for the deformation vector, another parameter σ is introduced. σ stands for the standard deviation of the intensity difference between the reference subset and the target subset. It controls the weights of the intensity difference. A large σ signifies minor difference of the whole weight matrix. On the contrary, a small one means a sharp appearance of the Gaussian kernel. Apparently, σ affects the anti-noise property of KDIC. More details about the choice of σ are given in the following section.

3. Simulation Analysis

In order to validate the effectiveness of the new KDIC method proposed in this paper, synthetic speckle images [18], with the deformation parameters already known, are produced to analyze the deformation of the specimen and evaluate the results of this new method more objectively. The reference simulation image is generated by the computer randomly, shown in Figure 1. The parameters of the simulated image are listed as: the size of the speckle images is 256×256pixels, the number of the speckles is 2000, and the size of the speckles is 4 pixels. Then, based on the reference image, twenty deformation images are generated with 0.05 pixel displacement increment along y direction. After that, noise with 1%, 2% and 4% levels is separately added to this group of images whose displacements range from 0-1pixel. So, four sets of images are gotten. The speckle image with 4% noise level is shown in Figure 1.

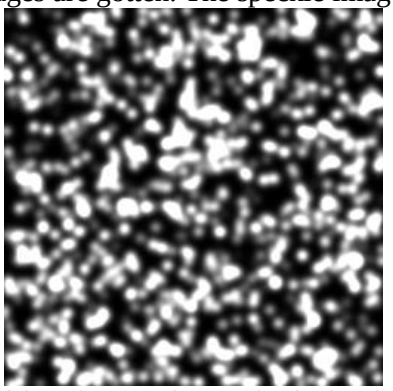

(a) Reference image (Noiseless)

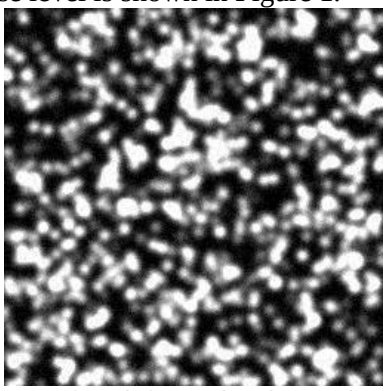

(b) Image after deformation (4% noise level)

Figure 1. Simulated Speckle Images

Before a further research, key parameter σ should be determined firstly. It associates with the Gaussian kernel shape, displayed in Figure 2. According to the analysis of the noiseless speckle images, intensity differences of the reference subset and the target subset are at subpixel level when Eq.3 converged. However, for noisy images, the intensity differences are basically lager than 1, some even greater than 10. As to these large differences, smaller weights, near to zero, should be given to them to reduce the influence of the noise. And large weights are encouraged for these small intensity differences.

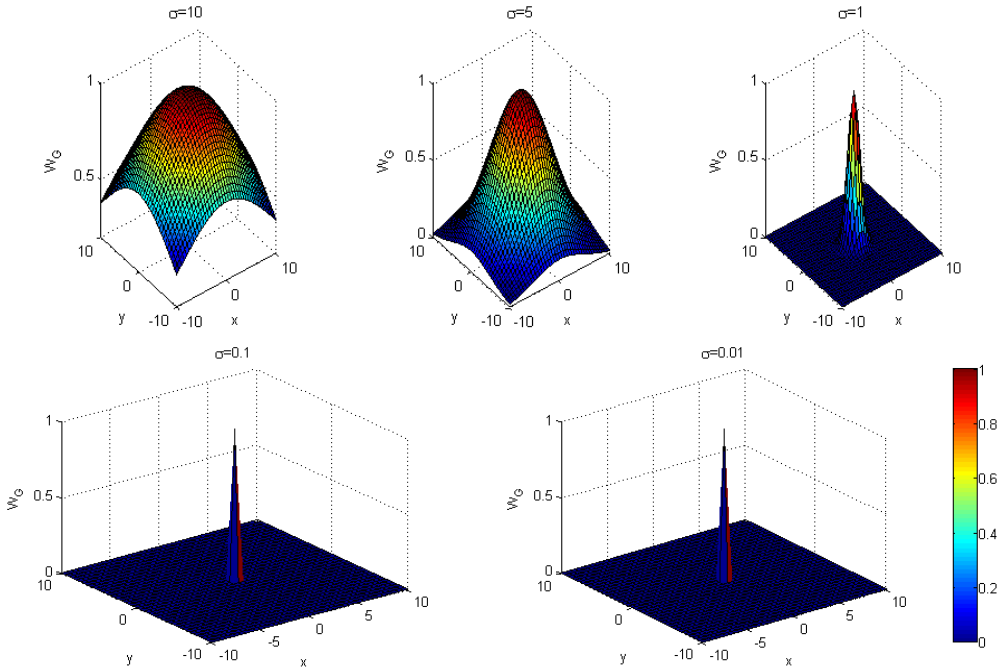

Figure 2. Gaussian Kernel Shape at Different Bandwidths

According to the reference [14], bias errors of the displacements ranging from 0-1 pixel are distributes sinusoidally, maximized at displacement 0.2 and 0.8 nearby. So, speckle image with displacement 0.2 and noise level 2% is analyzed for an optimal bandwidth selection. Displacements are estimated by TDIC and KDIC (with different bandwidths), and bias errors, defined in Eq.16, of the two techniques are shown in Figure 3.

$$e_v = \bar{v} - v_{true} \qquad (16)$$

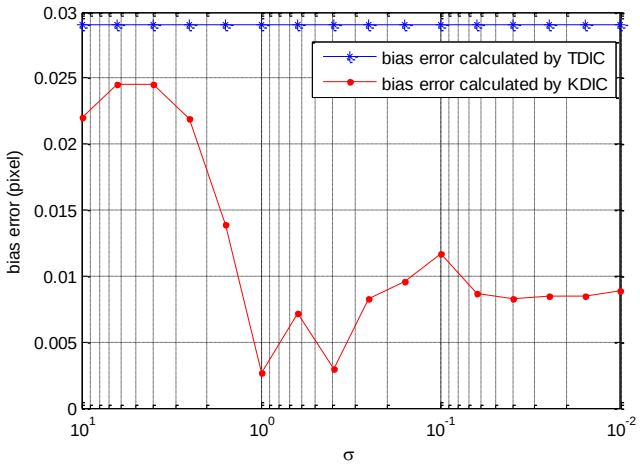

Figure 3. Bias Errors Calculated by TDIC and KDIC

From Figure 3 we can get, (1) Compared with TDIC, KDIC can effectively reduce the bias error of the displacement estimation at true displacement 0.2; (2) For KDIC, bandwidth less than 1, that is to say, bandwidth at subpixel, is more excellent for bias error reduction. And bandwidths ranging from 0.1-0.01 bring analogous effect. Obviously, bandwidth at 0.5 nearby help gains optimal result. Similar results can be gotten for other displacements. This corresponds to the analysis above. True intensity differences of the two subsets, not including noise, are at subpixel. Hence, recommended bandwidth, which represents the standard deviation of the intensity differences, is at subpixel too. And, optimal bandwidth is about 0.5 for reference.

Different noise levels may have different impact on the displacement calculation obtained via traditional DIC. Four sets of images (noiseless, 1% level, 2% level, 4% level), with true displacements ranging from 0-1pixel, are dealt with TDIC. The calculated displacements are evaluated with two indexes, which are mean bias error (defined in Eq.16) and standard deviation error. The expression of the latter is shown as:

$$\sigma_v = \sqrt{\frac{1}{N-1}\sum_{i=1}^{N}(\mathrm{v}_i - \bar{v})^2} \qquad (17)$$

Where $\bar{v}$ stands for the mean value of all the grid point displacements in one deformation image, that is to say, $\bar{v} = \frac{1}{N}\sum_{i=1}^{N} v_i$; v_{true} is the true displacement of the simulated image; N presents the number of all the grid points.

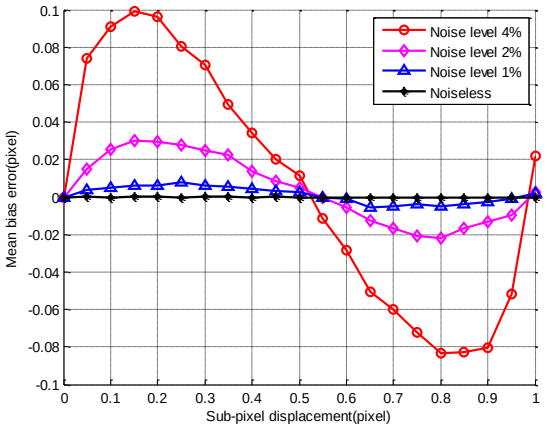

Figure 4. Mean Bias Errors of the Displacements Calculated by TDIC of the Four Image Sets

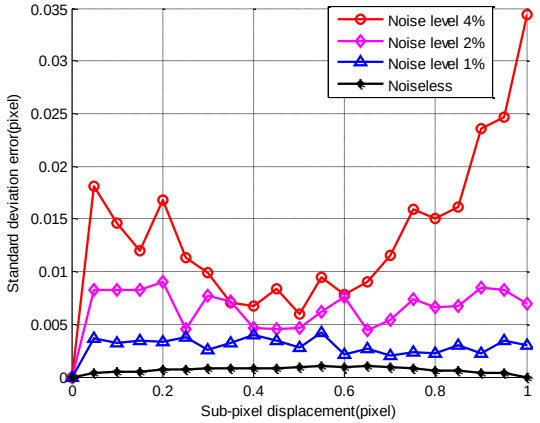

Figure 5. Standard Deviation Errors of the Displacements Calculated by NR of the Four Image Sets

Figure 4 and Figure 5 show the mean bias errors and standard deviation errors of the displacements calculated by TDIC separately. From Figure 4 we can see that, with the increment of the noise level, effects on the displacements become more apparently. The higher the noise level is, the bigger the two errors are. For the maximum mean bias error, it increases from 0.0077pixel to 0.0994pixel. Similarly, Figure 5 shows that the standard deviation error increases from 0.0029pixel to 0.0133pixel with the raise of the noise levels.

Then, kernel based DIC presented in this paper is applied to deal with the four simulated image sets. And the two kinds of errors are calculated and listed in Figure 6 and Figure 7.

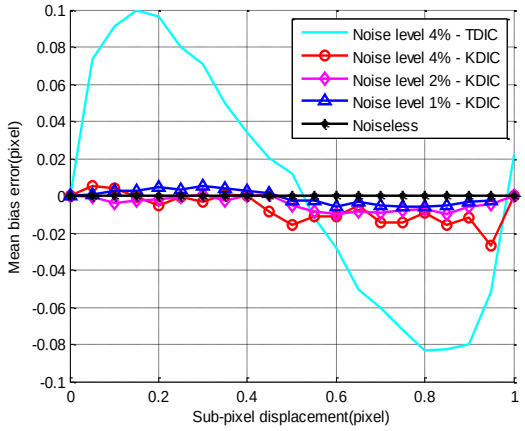

Figure 6. Mean Bias Errors of the Displacements Calculated by KDIC of the Four Image Sets

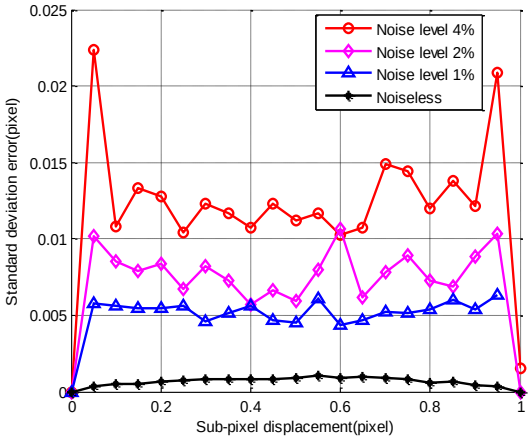

Figure 7. Standard Deviation Errors of the Displacements Calculated by KDIC of the Four Image Sets

As shown in Figure 6, compared with the displacement mean bias error of 4% noise level calculated by TDIC, the displacement errors of the four image sets calculated by KDIC are all dramatically reduced. For example, as for images with 4% noise level, the maximum error decreases from 0.094pixel to 0.0271pixel, which validates the remarkable effectiveness of the new KDIC method.

Maximum mean bias errors and standard deviation errors of the four image sets are listed in Table 1 in detail. The results demonstrate the effectiveness of the KDIC method to decrease the mean bias error. However, to some extent, there is no improvement for reducing the standard deviation error of the displacement calculation. For 1% noise level, which means the SNR (Signal to noise ratio) of the image is 40dB, the maximum mean bias error of the displacement calculation is 6‰. For the industrial cameras, the SNR values can reach 40dB and some may be higher. So, for practical use, precision with 1‰ of the KDIC method can satisfy the requirement of the high-precision displacement calculation.

Table 1. Maximum Bias Errors and Standard Deviation Errors of TDIC and KDIC Calculation

Noise level	Maximum bias error calculated by TDIC (L) and KDIC (R)	Mean SD error calculated by TDIC (L) and KDIC (R)
0	0.00027/-	0.00065/-
1%	0.0077/0.0062	0.0029/0.0048
2%	0.0302/0.0097	0.0064/0.0072
4%	0.0994/0.0271	0.0133/0.0119

4. Experimental Verification

For verifying the validity of the KDIC method to process the practical collected images, results calculated by KDIC are analyzed in the following. The specimen is displaced in Fig 8, which is made of aluminum with rivets in it. Usually, strain of the regions around the rivets can not be detected by strain gages directly. So, this new kind of full-field and non-contact KDIC method shows advantages for strain measurement. The images of the specimen are acquired in a uniaxial tensile test in y direction continuously. Some of the images at different collected times are dealt by KDIC.

Displacements obtained by KDIC are differentiated to get strain distribution and the strain changing processes are shown in Fig 9. When the specimen is stretched upwards with the bottom of the specimen fixed, regions on the specimen under the rivets are affected by stress concentration, and the results in Fig 9 are consistent with the theoretical analysis, which undoubtedly prove the effectiveness and feasibility of the KDIC method in practical experiment.

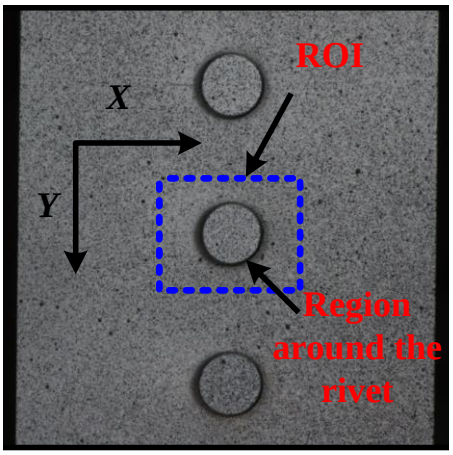

Figure 8. Image of the Specimen

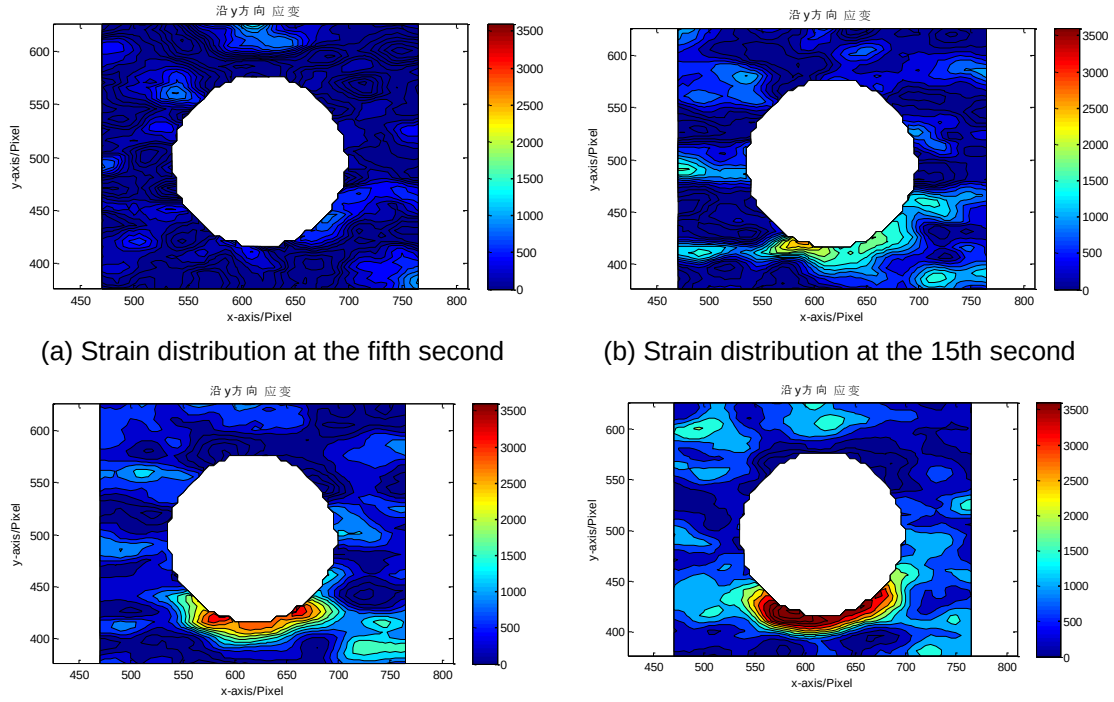

(a) Strain distribution at the fifth second

(b) Strain distribution at the 15th second

(c) Strain distribution at the 25th second

(d) Strain distribution at the 35th second

Figure 9. Strain Distribution around the Region of the Rivets

5. Conclusion

In conclusion, considering bad effects of the random image noise on the displacement calculated by TDIC, a kernel based DIC method which is a generalization expression of TDIC, is proposed in this paper to improve the robustness of DIC without sacrificing the intensity gradient. As for large intensity differences caused by noise, smaller weights, near to zero, should be given to them to reduce the influence of the noise. And large weights are encouraged for these small intensity differences. Obviously, KDIC is a novel method for bias error reduction without changing the image information. Both the simulation analysis and the experimental results verify the effectiveness of KDIC to reduce the bias error for a high-precision displacement calculation.

Acknowledgements

This work was supported by the Aeronautical Science Foundation of China (Grant No. 20120952022) and the Fundamental Research Funds for the Central Universities (Grant No. NS2014020)

References

[1] M A. Sutton, J J. Orteu and H W. Schreier, "Image correlation for shape, motion and deformation measurements", J. Springer, New York, vol. 10, (**2009**), p. 978-0.
[2] B. Pan, K. Qian and H. Xie, "Two-dimensional digital image correlation for in-plane displacement and strain measurement: a review", J. Measurement science and technology, vol. 20, no. 6, (**2009**), p. 062001.
[3] F. Pierron, M A. Sutton and V. Tiwari, "Ultra high speed DIC and virtual fields method analysis of a three point bending impact test on an aluminium bar", J. Experimental mechanics, vol. 51, no. 4, (**2011**), pp. 537-563.

[4] Y. Zhou and Y Q. Chen, "Propagation function for accurate initialization and efficiency enhancement of digital image correlation. J. Optics and Lasers in Engineering, vol. 50, no. 12, (**2012**), pp. 1789-1797.
[5] B. Pan, K. Li and W. Tong, "Fast, robust and accurate digital image correlation calculation without redundant computations", J. Experimental Mechanics, vol. 53, no. 7, (**2013**), pp. 1277-1289.
[6] C C B. Wang, J M. Deng and G A. Ateshian, "An automated approach for direct measurement of two-dimensional strain distributions within articular cartilage under unconfined compression", J. Journal of Biomechanical Engineering, vol. 124, no. 5, (**2002**), pp. 557-567.
[7] J. Zhao, P. Zeng, and B. Pan, "Improved Hermite finite element smoothing method for full-field strain measurement over arbitrary region of interest in digital image correlation", J. Optics and Lasers in Engineering, 2012, vol. 50, no. 11, (**2012**), pp. 1662-167.
[8] Y Q. Wang, M A. Sutton, and H A. Bruck, "Quantitative error assessment in pattern matching: effects of intensity pattern noise, interpolation, strain and image contrast on motion measurements", J. Strain, vol. 45, no. 2, (**2009**) pp. 160-178.
[9] P. Lava, S. Cooreman and D. Debruyne, "Study of systematic errors in strain fields obtained via DIC using heterogeneous deformation generated by plastic FEA", J. Optics and Lasers in Engineering, vol. 48, no. 4, (**2010**), pp. 457-468.
[10] Y. Zhou, C. Sun and J. Chen, "Adaptive subset offset for systematic error reduction in incremental digital image correlation", J. Optics and Lasers in Engineering, vol. 55, (**2014**), pp. 5-11.
[11] Y. Yuan, J. Huang, and X. Peng, "Accurate displacement measurement via a self-adaptive digital image correlation method based on a weighted ZNSSD criterion", J. Optics and Lasers in Engineering, vol. 52, (**2014**), pp. 75-85.
[12] W. Tong, "Subpixel image registration with reduced bias [J]", Optics letters, vol. 36, no. 5, (**2011**), pp. 763-765.
[13] B. Pan, "Bias error reduction of digital image correlation using Gaussian pre-filtering", J. Optics and Lasers in Engineering, vol. 51(, no. 10, (**2013**), pp. 1161-1167.
[14] H W Schreier, J R Braasch and M A. Sutton, "Systematic errors in digital image correlation caused by intensity interpolation", J. Optical Engineering, vol. 39, no. 11, (**2000**), pp. 2915-2921.
[15] Z Y Wang, H Q Li and J W. Tong, "Statistical analysis of the effect of intensity pattern noise on the displacement measurement precision of digital image correlation using self-correlated images", J. Experimental Mechanics, vol. 47, no. 5, (**2007**), pp. 701-707.
[16] P. Mazzoleni, F. Matta, and E. Zappa, "Gaussian pre-filtering for uncertainty minimization in digital image correlation using numerically-designed speckle patterns", J. Optics and Lasers in Engineering, vol. 66, (**2015**), pp. 19-33.
[17] D. Comaniciu and P. Meer, "Mean shift: A robust approach toward feature space analysis", J. IEEE Transactions on Pattern Analysis and Machine Intelligence, vol. 24, no. 5, (**2002**), pp. 603-619.
[18] P. Zhou and K E. Goodson, "Subpixel displacement and deformation gradient measurement using digital image/speckle correlation (DISC)", J. Optical Engineering, vol. 40, no. 8, (**2001**), pp. 1613-1620.

Authors

Huan Shen, he received his Ph.D. degree from the Nanjing University of Aeronautics and Astronautics (NUAA) in 2010. Now he is a lecturer in NUAA. His research interests include image processing and pattern recognition.

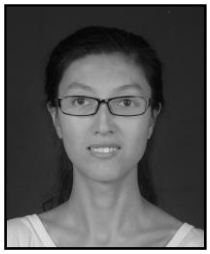

Peize Zhang, she is studying for a master's degree at the Nanjing University of Aeronautics and Astronautics. Her research interests include image processing and pattern recognition.

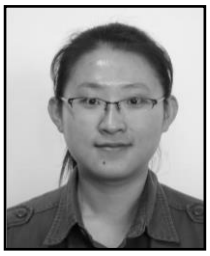

Xiang Shen, She is an engineer working in Aeronautics Science and Technology Key Laboratory of full scale aircraft structure and fatigue. Her research interest includes mechanical testing.